IMPACT OF MINING ACTIVITIES ON FOREST COVER LOSS IN THE CAVALLY RIVER WATERSHED

Manuscript Info

……..

Manuscript History
Received: xxxxxxxxxxxxxxx
Final Accepted: xxxxxxxxxxxx
Published: xxxxxxxxxxxxxxx

Key words:-
mining activities, forest cover degradation, watershed, cavally river.

Abstract

……

This study assesses the impact of mining activities on land use and vegetation cover degradation through the analysis of satellite imagery (LANDSAT, SENTINEL-2) over several years (1994, 2004, 2014, and 2024). The methodology used is supervised classification using the maximum likelihood algorithm. The results reveal a significant decline in vegetation cover (approximately -25%), accompanied by an increase in agricultural land (+18%), residential areas (+9%), and bare soils (+5%), reflecting accelerated anthropogenic pressure on the landscape. The classification accuracy, confirmed by Kappa coefficients ranging from 0.81 to 0.94 and overall accuracy between 86% and 94.4%, supports the reliability of the analyses. These spatial dynamics demonstrate a significant environmental impact of mining operations, with direct effects on natural ecosystems and indirect consequences related to urban expansion and land tenure pressures. The findings underscore the urgent need for sustainable land management strategies, including ecological restoration and effective regulation of mining expansion, to safeguard the environmental balance of affected areas.

Introduction:

Land cover constitutes a fundamental component of the ecological balance of terrestrial ecosystems. It plays a crucial role in climate regulation, soil conservation, biodiversity protection, and the maintenance of the hydrological cycle (FAO, 2020; IPBES, 2019). However, in many regions around the world, this natural capital is under severe threat from human activities, particularly mining. While mining is vital for economic development, it causes profound and often irreversible transformations of natural landscapes, including deforestation, soil stripping, and the alteration of both fauna and flora habitats (Sonter *et al.*, 2017; World Bank, 2023).

In developing countries, mineral resource extraction whether industrial or artisanal is often carried out in the absence of rigorous environmental planning. This greatly increases the risk of degradation of natural environments (Hilson & Van Bockstael, 2018). The rush for precious metals, especially gold, is frequently associated with extensive tree felling, soil leaching, sedimentation of watercourses, and the progressive disappearance of natural vegetation formations (VoxDev, 2023). These practices not only disrupt the structure of the vegetation cover but also compromise the ecosystem services it provides to local populations, such as water regulation, soil fertility, and non-timber forest resources (Millennium Ecosystem Assessment, 2005; UNEP, 2022).

The region of Ity, located in the western part of Côte d'Ivoire, shows this issue particularly well. Since the establishment of the Ity Mining Company in 1990, industrial mining activities combined with unregulated artisanal exploitation have significantly contributed to the degradation of vegetation cover within the Cavally River watershed (Fulgence *et al.*, 2020). The expansion of extraction zones, construction of access roads, storage of mining waste, and the proliferation of informal gold mining sites have led to widespread fragmentation of forest landscapes, threatening the ecological integrity of the region (ISS Africa, 2024; Earthworm Foundation, 2023).

In this context, the present study aims to assess the extent of vegetation cover degradation induced by mining activities in the Ity sub-watershed of the Cavally River. The research draws upon field observations, satellite

imagery, and geospatial analyses to measure land use change dynamics and to formulate recommendations for improved environmental management in areas under intense extractive pressure.

I. Materials and Methods

I.1. Study Area Presentation and Location

The Cavally River watershed is a transboundary basin located between longitudes 8°4′ and 7°7′ West, and latitudes 6°8′ and 7°9′ North. The Cavally River originates in Guinea, north of Mount Nimba, at an altitude of approximately 600 metres. Spanning a length of 700 km, the river serves as a natural boundary between Côte d'Ivoire and Liberia along its middle and lower courses (Girard *et al.*, 1967).

The sub-watershed investigated in this study is located in the Tonkpi region, specifically between the departments of Zouan-Hounien and Blolequin, in the vicinity of the Ity Mining Company. It lies between longitudes 8°1′30″ and 8°10′30″ West, and latitudes 6°56′25″ and 6°46′25″ North, as illustrated in Figure 1.

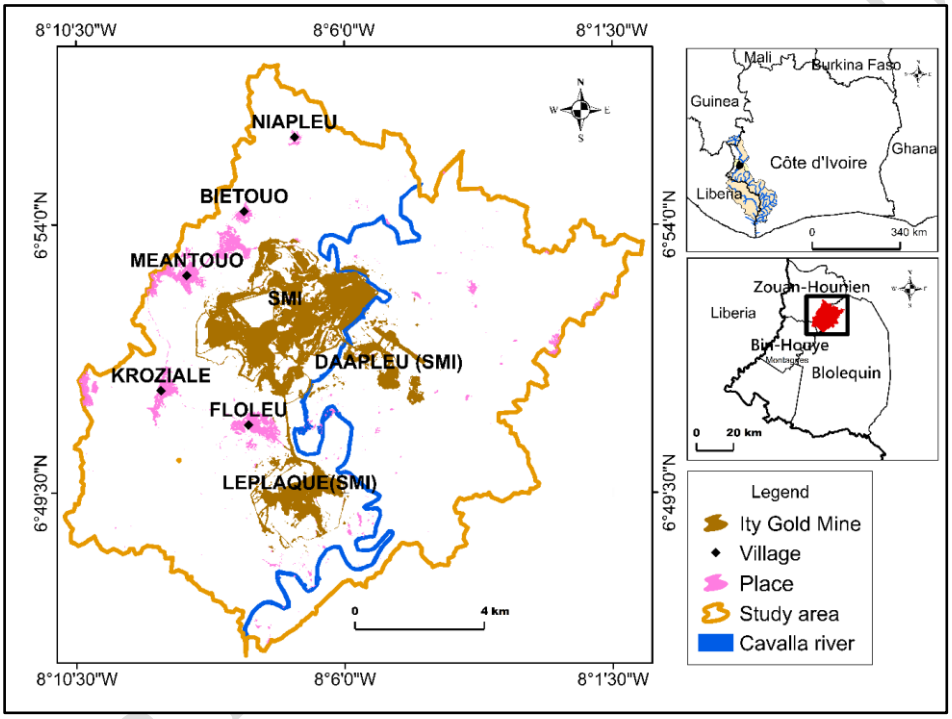

Figure 1 : Study area

I.2 Land Use and Land Cover Data

The data used to assess land use and land cover (LULC) dynamics consist of satellite imagery (LANDSAT and SENTINEL-2) as well as cartographic data.

The study is based on four satellite images acquired from the MSI-L2A, MSI-L1C, ETM+, and TM sensors. Two of these images are from LANDSAT satellites: scene 199-55 acquired on 27 December 1994 by the TM sensor on Landsat 5, and one captured on 30 January 2004 by the ETM+ sensor on Landsat 7. The other two images are from Sentinel-2: one acquired on 23 December 2014 by the MSI-L1C sensor, and another on 21 December 2023 by the MSI-L2A sensor.

All images were acquired between December and February, corresponding to the dry season, which helps minimise cloud cover. Moreover, dry season imagery offers better contrast between vegetation cover and other land use types, thereby improving classification accuracy.

Table I presents the main characteristics of the satellite images used in the study area (satellite name, date of acquisition, spatial resolution, etc.).

Table I: Characteristics of Sentinel-2 and Landsat images for the study are

Characteristics	Sensors			
	MSI L2A	MSI L1C	ETM	TM
Image Format	JPEG 2000	JPEG 2000	GEOTIFF	GEOTIFF
Satellite	SENTINE 2L2A	SENTINEL2L1C	LANDSAT7	LANDSAT5
Acquisition Date	21/12/2023	23/12/2014	30/01/2004	27/12/1994
Scene dimensions	110x110 km²	110x110 km²	185x185 km²	185x185 km²
Spatial resolution (XxY)	20mx20m	20mx20m	30mx30m	30mx30m
Projection	UTMZONE 29N	UTMZONE 29N	UTMZONE29N	UTMZONE29N
Data Sources	COPERNICUS	COPERNICUS	USGS	USGS

I.2.1 Data Processing and Analysis Methods

Data processing and analysis focused primarily on image processing and the use of a geospatial database within a GIS environment. The techniques applied combined remote sensing and Geographic Information System (GIS) methodologies.

I.2.2 Pre-processing

Image processing began with radiometric and atmospheric corrections. Radiometric correction enhances the reflectance values of pixels, while atmospheric correction reduces the effects of cloud cover and Harmattan dust (Song et al., 2001). In this study, image enhancement techniques were applied to improve image dynamics and increase the contrast between land cover classes and their surrounding environment.

For the purposes of land use and land cover analysis and mapping, five thematic classes were identified based on false-colour composites.

These pre-processing steps culminated in image classification, which involves converting spectral information contained in the satellite imagery into land use and land cover maps.

I.2.3 Supervised Classification

Unsupervised classification, combined with field surveys, was initially used to update the land cover classes and training samples. The supervised classification process involved the integration of 64 updated training classes into the composite bands of the satellite imagery. This classification technique was selected because of its high performance and suitability for generating land use and land cover maps (E. Fotsing, 2009; K. E. Konan, 2008).

The algorithm applied was the Maximum Likelihood Classifier, based on a Bayesian probabilistic approach, which assumes that the spectral responses of land cover classes follow a Gaussian distribution. Pixels are then assigned to the class for which they have the highest probability of membership (R. Caloz & C. Collet, 2001).

The classified images were evaluated using overall accuracy and the Kappa coefficient, and further validated through a field verification campaign. This campaign ensured the thematic accuracy of the classified images by comparing them with ground-truth data. The training dataset was continuously updated by combining field data with historical satellite imagery and Google Earth archives for the years 1994, 2004, and 2014.

To improve thematic coherence and eliminate isolated pixels, a 3×3 median filter was applied to the classified images. The homogenised classification results were then vectorised and integrated into a Geographic Information System (GIS) for further management and spatial analysis. This process enabled the production of land use and land cover maps and associated statistics for the years 1994, 2004, 2014, and 2024.

II. Results

II.1 Validation of Land Use and Land Cover Maps

Following the processing of satellite imagery, land use and land cover (LULC) maps were generated for the entire study period. The classification results were validated using the Kappa coefficient, calculated from the confusion matrices.

The results indicate that the Kappa coefficient for all years considered ranges between 0.81 and 0.94, with an overall accuracy varying from 86% to 94.4%.

The confusion matrices and corresponding Kappa values are presented in Tables II, III, IV, and V.

The confusion matrix for the 1994 land cover classification shows that a total of 68 pixels were evaluated. Of these, 59 pixels in the 1994 classified map matched those in the reference image, resulting in an overall accuracy of approximately 86.76%.

Table II: Confusion matrix for the 1994 Landsat TM classificationOverall Accuracy: 88%, Kappa: 0.83

		Reference data (field observation)						
		Water	Building	Bare soil	Vegetation	Crops	Total	Percentage
Classified data (interpreted images)	Water	**21**	0	1		0	22	95,45
	Building	0	**9**	0	1	0	10	90
	Bare soil	1	0	**4**	1	2	8	50
	Vegetation	1	0	0	**16**	0	17	94,12
	Crops	0	0	0	2	**9**	11	81,82
	Total	23	9	5	20	11	68	
	Percentage	91,30	100	80,00	80	81,82		

In Table III, 69 classified pixels are compared with those from the reference image. Among them, 59 pixels — representing approximately 85.51% — show good agreement.

Table III: Confusion matrix for the classification of the 2004 Landsat ETM+ imageOverall Accuracy: 86%**,** KappaCoefficient: 0.81

		Reference data (field observation)						
		Water	Building	Bare soil	Vegetation	Crops	Total	Percentage
Classified data (interpreted images)	**Water**	21	0	0	0	0	21	100,00
	Building	0	9	0	2	0	11	81,82
	Bare soil		0	4	0	2	6	66,67
	Vegetation		2	1	16	1	20	80,00
	Crops	0	0	1		9	11	81,82
	Total	21	11	6	19	12	69	
	Percentage	100	81,82	66,67	84,21	75		

With regard to the 2014 land cover classification, a total of 66 pixels were tested to assess its accuracy, of which 59 pixels were correctly classified, resulting in an overall accuracy of 89.39% (Table IV).

Table IV: Confusion matrix for the classification of the 2014 Sentinel2 L1C imageOverall Accuracy: 88%, Kappa Coefficient: 0.86

		Reference data (field observation)						
	Classes	Water	Building	Bare soil	Vegetation	Crops	Total	Percentage
Classified data (interpreted images)	Water	21		1	1		23	91,30
	Building	0	9	0	1	0	10	90
	Bare soil	0	0	4	0	2	6	66,67
	Vegetation			0	16	2	18	88,89
	Crops	0	0	0		9	9	100,00
	Total	21	9	5	18	13	66	
	Percentage	100	100	80	88,89	69,23		

For the 2024 image, a total of 63 pixels were evaluated. Among these, 60 pixels from the 2024 classified map were consistent with those in the reference image, resulting in an overall accuracy of 95.23%.

Table V: Confusion matrix for the classification of the 2024 Sentinel-2A imageOverall Accuracy: 94.4%, Kappa Coefficient: 0.94

		Reference data (field observation)						
		Water	Building	Bare soil	Vegetation	Crops	Total	Percentage
Classified data (interpreted images)	Water	21	0		0	0	21	100,00
	Building	0	10	0	0	0	10	100
	Bare soil	0	1	4	0	0	5	80
	Vegetation		0	1	16	1	18	88,89
	Crops	0	0	0		9	9	100,00
	Total	21	11	5	16	10	63	
	Percentage	100	90,91	80	100	90		

II.2. Land Use and Land Cover Status in 1994, 2004, 2014 and 2024

In 1994, the watershed was predominantly covered with natural vegetation, particularly in the central part, extending from the upstream to the downstream sections. The western part of the study area was mainly occupied by agricultural land, while the eastern portion was characterised by the dominance of bare soils.

By 2004, a significant conversion of natural vegetation into croplands was observed in the central part of the basin. In addition, agricultural areas in the west were progressively replaced by built-up areas (settlements) and bare soils.

In 2014, there was a marked expansion of built-up areas in the western part of the watershed, along with a general increase in bare soil coverage across the entire study area.

By 2024, built-up areas and bare soils continued to expand, particularly in the central and western parts of the basin, indicating an intensification of anthropogenic pressure and a probable degradation of natural vegetation cover.

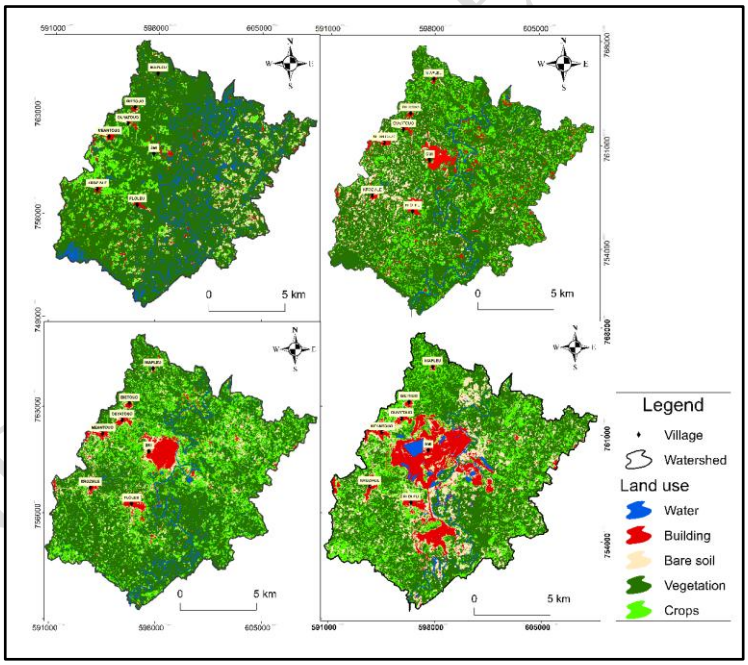

Figure 2: Maps showing the spatio-temporal dynamics of land use and land cover from 1994 to 2024: A–1994, B–2004, C–2014, D–2024.

II.3. Land Use and Land Cover Dynamics between 1994, 2004, 2014 and 2024

The analysis of Table VI reveals a significant evolution in land use and land cover within the watershed over the period 1994–2024. In 1994, vegetation covered the majority of the area, with an estimated surface of 130 ha,

representing 77.45% of the total area. This vegetative cover gradually declined, reaching 115.31 ha (68.70%) in 2004, 98.88 ha (58.91%) in 2014, and 82.89 ha (49.39%) in 2024. This decline reflects a continuous loss of dense forest or natural vegetation, likely associated with mining activities in the region.

This reduction occurred in favour of agricultural areas, built-up zones, and bare soils. Cultivated land accounted for 9.65 ha (5.75%) in 1994, expanded significantly to 26.52 ha (15.80%) in 2004, and further to 41.23 ha (24.62%) in 2014, before slightly decreasing to 33.95 ha (20.23%) in 2024.

Urbanised areas and bare soils exhibited a contrasting trend. Their combined area decreased slightly between 1994 and 2014, from 25.11 ha (14.96%) in 1994 to 22.58 ha (13.45%) in 2004, and to 21.21 ha (12.64%) in 2014. However, this trend reversed sharply between 2014 and 2024, with a notable increase to 46.40 ha (27.65%).

These spatial dynamics, derived from remote sensing data, reflectincreasing pressure on the watershed's natural resources**,** driven bymining expansion**,** agricultural intensification, andurbanisation**,** all occurring at the expense of vegetated areas.

The surface areas (in hectares) of the Ity Mining Company (SMI)andbare soilsare provided inTable VI**.**

Table VI: Land cover class areas (in hectares) from 1994 to 2024

Classes	1994		2004		2014		2024	
Water	309,11	1,84	344,06	2,05	642,82	3,83	459,87	2,74
Building	557,21	3,32	896,36	5,34	822,39	4,90	1962	11,69
Bare soil	1953,31	11,64	1361,33	8,11	1299,05	7,74	2678,05	15,96
Vegetation	13000,32	77,45	11531,45	68,70	9888,63	58,91	8289,77	49,39
Crops	965,05	5,75	2651,8	15,80	4132,11	24,62	3395,31	20,23
Total	**16785**	**100**	**16785**	**100**	**16785**	**100**	**16785**	**100,00**

II.4 Assessment of Vegetation Cover Degradation between 1994 and 2024

Figure 3 highlights a marked degradation of vegetation cover, with a loss of nearly 25% of the initial surface area. This decline has occurred in favour of the expansion of agricultural areas (18%), built-up areas (15%), and bare soils (5%), reflecting a significant environmental degradation largely associated with mining activities.

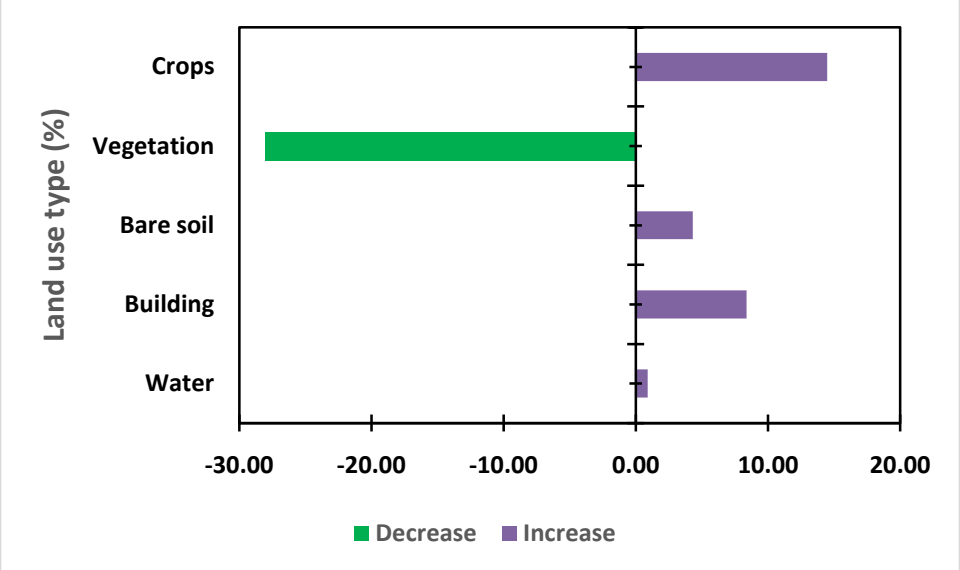

Figure 3: Percentage of land use units between 1994 and 2024

III. Discussion

The results obtained show Kappa coefficients ranging from 0.81 to 0.94, and overall classification accuracies between 86% and 94.4%, indicating a very high quality of the classified images used in the land use and land cover analysis. These values are well above the 0.75 threshold, which is considered excellent according to Landis & Koch (1977), and confirm the reliability of the datasets used to assess environmental dynamics in the study area.

The significant decline in vegetation cover observed is consistent with numerous studies that have documented the impact of mining activities on tropical forest ecosystems. For instance, Acheampong et al. (2022) reported that mining zones in Ghana experienced more than 30% vegetation loss over two decades, largely due to illegal gold mining and urban expansion. Similarly, Béland et al. (2021) highlight that both artisanal and industrial mining are major drivers of deforestation in West Africa.

Moreover, the observed increase in agricultural land, built-up areas, and bare soils reflects a rapid process of landscape anthropisation, a dynamic commonly found around mining basins. According to Hilson & van der Vorst (2023), the establishment of mining operations attracts large populations, thereby increasing the demand for housing, infrastructure, and farmland, which accelerates the conversion of natural areas.

The slight increase in water surface area may be explained by the creation of retention ponds or hydrological disturbances caused by mining activities, as shown by Niane et al. (2020) in Guinea. Such changes in the hydrological landscape heighten the risks of water pollution and disruption of aquatic ecosystems.

Conclusion

The analysis of land use and land cover dynamics, supported by high-accuracy classification (Kappa coefficient ranging from 0.81 to 0.94; overall accuracy between 86% and 94.4%), reveals a marked transformation of the landscape driven by mining activities. The significant decline in vegetation cover, alongside the expansion of agricultural areas, built-up zones, and bare soils, reflects a process of accelerated anthropisation and a notable degradation of natural ecosystems.These findings confirm that mining operations constitute a major driver of environmental pressure not only through the direct destruction of natural habitats, but also through the indirect dynamics they trigger, such as population growth, urban sprawl, and land use conversion. The disruption of ecological balances is therefore evident, with potential consequences for biodiversity, water resources, soil fertility, and the livelihoods of local populations.

References

1 Acheampong, E.O., et al. (2022). Mining and deforestation: An assessment of the environmental impact inGhana. *Environmental Monitoring and Assessment*, 194(6), 123.

2 Béland, M., et al. (2021). Mining and land use change in West Africa: A systematic*review*. Land Use Policy, 107, 105479.

3 Caloz Régis et Collet Claude, (2001). Traitements numériques d'image en télédétection. Précis de télédétection, vol. 3, Agence universitaire de la francophonie (AUF) et Presses de l'université du Québec, Montréal.

4 Earthworm Foundation. (2023). Projet Cavally : un exemple de restauration forestière durable en Côte d'Ivoire.

5 FAO. (2020). Global Forest Resources Assessment *2020*. Rome.

Fotsing Eric, (2009). SMALL Savannah : Un système d'information pour l'analyse intégrée des changements d'utilisation de l'espace à l'extrême nord du Cameroun, (S.l.), Universiteit Leiden.

6 Fulgence, B. et al. (2020). Influence of Mining on the Ecological Quality of the Cavally River, Western Côte d'Ivoire. INNSPUB.

7 Girard, J Sircoulon, & P., T. (1967). Aperçu sur les régimes hydrologiques.

8 Hilson, G., & Van Bockstael, A. (2018). Artisanal mining and rural livelihoods in Africa: Change, challenges and policy options. *Resources Policy*, 59, 43–53.

9 Hilson, G., & van der Vorst, R. (2023). Mining, migration and development in Sub-Saharan Africa. *Resources Policy*, 83, 103657.

10 IPBES. (2019). Global Assessment Report on Biodiversity and Ecosystem Services.

11 ISS Africa. (2024). Côte d'Ivoire's mines risk degrading its fragile environment.

12 Konan Kouadio Eugène, (2008). Conservation de la diversité végétale et activités humaines dans les aires protégées du sud forestier ivoirien : L'exemple du Parc National d'Azagny. Université de Cocody-IGT.

13 Landis, J.R., & Koch, G.G. (1977). The measurement of observer agreement for categorical data. *Biometrics*, 33(1), 159–174.

14 Millennium Ecosystem Assessment. (2005). Ecosystems and Human Well-being: Synthesis.

15 Niane, B., et al. (2020). Hydrological impacts of artisanal mining in Guinea. *Hydrology Research*, 51(4), 655–668.
16 Song C., Curtis E. W., Karen C. S., Mary P. L., et Scott A. M. (2001). Classification and change detection using Landsat TM data: When and how to correct atmospheric effects? *Remote Sens. Environ.* 75, p. 230-244.
17 Sonter, L. J., Barrett, D. J., Moran, C. J., & Soares-Filho, B. S. (2017). Mining drives extensive deforestation in the Brazilian Amazon.*Nature Communications*, 8(1), 1013.
18 UNEP. (2022). State of the Environment Report 2022.
19 VoxDev. (2023). The role of artisanal mining in deforestation: New insights from Africa-wide data.
20 World Bank. (2023). The World Bank Group's Evolution Roadmap: Supporting Green, Resilient, and Inclusive Development.